Faraday rotation in a disordered medium

V. Gasparian[1] and Zh. S. Gevorkian[2,3,*]

[1]*California State University, Bakersfield, California 93311-1022, USA*

[2]*Yerevan Physics Institute, Alikhanian Brothers Street, 2,0036 Yerevan, Armenia*

[3]*Institute of Radiophysics and Electronics, Ashtarak-2, 0203, Armenia*

(Received 20 October 2012; published 6 May 2013)

The Faraday rotation angle Θ is calculated in a diffusive regime on a three-dimensional disordered slab. It is shown that $\tan\Theta$ is (i) an oscillating function of the magnetic field or the medium's internal properties, and (ii) proportional to the ratio of the inelastic mean-free path $l_{\rm in}$ to the mean-free path l, that is, to the average number of photon scatterings. The maximum rotation is achieved at frequencies when the photon's elastic mean-free path is minimal. We have obtained the rotation angle of backscattered light taking into account the maximally crossed diagrams. The latter leads to an ellipticity in the backscattered wave that can serve as a precursor of weak localization. The critical strength of the magnetic field is $B_c \sim g_c \sim \lambda/l$ beyond which rotation in the backscattered wave disappears. The traversal time of an electromagnetic wave through the slab is estimated in a diffusive regime. The disorder enhanced the traversal time by an additional factor $l_{\rm in}/l$ in comparison with a free light propagation time. Comparison with the experimental data is carried out.

DOI: 10.1103/PhysRevA.87.053807 PACS number(s): 42.25.Dd, 41.20.Jb, 71.45.Gm, 71.55.Jv

I. INTRODUCTION

Since Anderson's pioneering paper [1] where the concept of localization of an electron moving in a random potential was introduced, propagation of electromagnetic waves through disordered media have been attracting a lot of interest (see, for example, Ref. [2] and references therein). One of the reasons for such interest is the possibility of observing weak-localization effects in disordered systems. Most of the papers were devoted to the backscattering peak where weak-localization effects are manifest (see, e.g., Refs. [3–7] and, for a recent experiment, Ref. [8]). The influence of polarization effects on the backscattering peak was investigated in Ref. [9]. Along with the transport properties of disordered media, magneto-optical effects in such systems capture broader attention. Particularly, in Ref. [10], the light backscattering peak in parity-non-conserving disordered media was investigated. In such a medium, rotation of the polarization plane is possible.

A Faraday rotation is a magneto-optical phenomenon that rotates the polarization of light. It occurs as an internal property of the medium as well as under the external magnetic field. In both cases, the dielectric permittivity tensor of the system becomes anisotropic. For example, in a GaAs crystal, large Faraday rotation [11] originates because of the spin-orbit coupling. Faraday rotation is observed in astronomy. There, it is used for measurement of magnetic fields [12].

In the past decade, many experimental papers [13–18] have been devoted to the Faraday rotation in disordered media. In Refs. [15–18], attention was drawn to the fact that a large enhancement of the Faraday rotation can be obtained in nanomaterials incorporating several nanoparticles and their composites. A garnet composite film (mostly a Bi-substituted yttrium iron garnet) incorporating gold nanoparticles or a nanoparticles solution with gold-coated Fe_2O_3 [15–18] show a change in the sign of the Faraday rotation at the wavelengths corresponding to the surface-plasmon absorption peak of the gold nanoparticles. Around the local surface-plasmon resonance wavelengths, a resonant transmittance attenuation and a large resonant enhancement of the Faraday rotation with a narrow bandwidth was obtained in Ref. [15]. Recently, a large Faraday rotation was observed [19] in an ultrathin graphene film. The analogy with the Hall effect is revealed.

The standard effective medium approximations (Maxwell-Garnett and Bruggeman theories) [20] describe the macroscopic properties of a medium using the average dielectric constant determined by the relative fractions of its components. These theories show only qualitative agreement with the experimental data of Refs. [15–18]. Many of the questions that have been raised during the experiments are still waiting for answers. For example, so far, no corresponding analytical calculation has been available for a discrepancy in the bandwidth between the transmission attenuation and the resonant Faraday rotation (Ref. [15]). Of particular importance is the influence of the disorder, induced by the presence of the impurities, on the Faraday angle and on several related quantities.

In the present paper, we develop a theoretical approach for investigating the Faraday rotation for transmitted and backscattered waves in three-dimensional disordered media. We show that the maximum Faraday rotation angle of the transmitted wave is achieved at the frequencies where the photon elastic mean-free path is minimal. In the backscattered wave, the maximally crossed diagram contribution to the Faraday rotation angle is very important. It leads to an ellipticity of the backscattered wave in the localized regime.

The paper is organized as follows. In Sec. II, we formulate the problem. The coherent-potential approximation is discussed in Sec. III, and the appropriate contribution to the Faraday angle is calculated. In Sec. IV, we present results for the diffusional contribution to the Faraday rotational angle. Diffusional and maximally crossed diagram contributions are taken into account for the Kerr effect in Sec. V. Obtained analytical results are compared with experimental data in Sec. VI. Finally, the main conclusions are summarized in Sec. VIII. The paper contains two appendices, which present some technical details useful for the understanding of diffusional

*gevork@yerphi.am

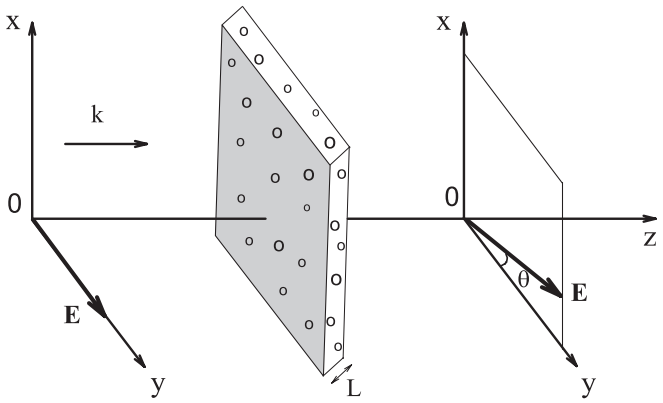

FIG. 1. Geometry of the problem. The incident wave is polarized on $0y$. After transmission through a slab, the polarization vector rotates.

and maximally crossed diagram contributions to the Kerr effect.

II. FORMULATION OF THE PROBLEM

Let us consider the incidence of a linearly polarized electromagnetic wave on the optically active medium, see Fig. 1. We assume that the incident field is polarized on $0y$, the plane of incidence is xz, and the wave vector is directed on $0z$. Because of the scattering, the transmitted field contains all the directions of the wave vector. In order to determine the Faraday angle, one should separate the coherent part, that is, the one directed on $0z$, see Fig. 1. The Faraday rotation angle is determined as follows:

$$\tan\,\Theta = \left\langle \frac{E_x}{E_y} \right\rangle, \tag{1}$$

where $E_{x,y}$ are the components of the transmitted coherent wave and $\langle\cdots\rangle$ means averaging over the realizations of randomness. The phases of the electric-field components are strongly fluctuating contrary to intensities. Therefore, for a weakly scattering medium, one can approximately take

$$\tan\,\Theta \approx \frac{\langle E_x E_y^* \rangle}{\langle E_y E_y^* \rangle}. \tag{2}$$

The Maxwell equation for the electric field has the form

$$\nabla^2 E_i(\vec{r}) + \varepsilon_{ij}(\vec{r})\frac{\omega^2}{c^2}E_j(\vec{r}) = j_i(\vec{r}), \quad \vec{\nabla}\cdot\vec{E} = 0, \tag{3}$$

where $\vec{j}$ is the source term and the dielectric tensor is determined as follows:

$$\varepsilon_{ij}(\vec{r}) = [1+\varepsilon(\vec{r})]\delta_{ij} - i e_{ijk}\mathbf{g}_k. \tag{4}$$

Here, e_{ijk} is the antisymmetric tensor, and $\mathbf{g}$ is the gyration vector directed on the magnetic-field direction when an external field is applied. In the optically active medium without an external field, $\vec{g} = f\vec{q}$ and is parallel to the direction of photon propagation. $\varepsilon(\vec{r})$ is the random part which is assumed Gaussian distributed with the δ-correlation function,

$$\langle \varepsilon(\vec{r})\varepsilon(\vec{r}')\rangle = \gamma\delta(\vec{r}-\vec{r}'). \tag{5}$$

In order to carry out averaging over the randomness, it is convenient to express all the quantities through the Green's functions,

$$\nabla^2 G^R_{ij}(\vec{r},\vec{r}') - \frac{\partial^2 G^R_{kj}(\vec{r},\vec{r}')}{\partial r_i \partial_k} + \varepsilon_{ik}(\vec{r})\frac{\omega^2}{c^2}G^R_{kj}(\vec{r}) = \delta_{ij}\delta(\vec{r}-\vec{r}'). \tag{6}$$

As was mentioned, the Faraday rotation angle in Eqs. (1) and (2) is determined by the coherent intensity. Hence, to separate the coherent intensities, let us introduce the intensity tensor at observation point $\vec{R}$ and in the direction of unit vector $\vec{s}$ following [9]:

$$I_{ij}(\vec{R},\vec{s}) = 2\int_0^\infty q^2 dq \int d\vec{r}\, e^{-iq\vec{s}\vec{r}} \times \langle E_i(\vec{R}+\vec{r}/2)E_j^*(\vec{R}-\vec{r}/2)\rangle. \tag{7}$$

Using Eq. (7), the Faraday angle Eq. (2) can be represented in terms of an intensity tensor $I_{ij}(\vec{R},\vec{s})$,

$$\tan\,\Theta \approx \frac{I_{xy}(L,\hat{\mathbf{s}}_z)}{I_{yy}(L,\hat{\mathbf{s}}_z)}. \tag{8}$$

Here, $\hat{\mathbf{s}}_z$ is the unit vector on z and L is the thickness of the slab. Because of the symmetry, the intensities depend only on the z coordinate.

III. COHERENT-POTENTIAL APPROXIMATION

Averaged Green's functions take into account the fact that the right-hand and the left-hand circular polarized lights see different refractive indexes in the medium [10],

$$G^{R,A}_{ij}(\vec{q}) = \sum_{\alpha=\pm1}\frac{\frac{1}{2}(\delta_{ij} - \hat{q}_i\hat{q}_j \mp i\alpha e_{ijm}\hat{q_m})}{(1-\alpha\hat{\mathbf{q}}\vec{\mathbf{g}})k_0^2 - q^2 \pm ik_0/l}, \tag{9}$$

where $k_0 = \omega/c$, $\hat{\mathbf{q}}$ is a unit vector on $\vec{q}$, and $l = 6\pi/\gamma$ is the photon elastic mean-free path. The superscripts R and A denote retarded and advanced Green's functions, respectively.

The Faraday angle consists of two main contributions. One comes from the coherent-potential approximation, and the other comes from the diffusional scattering of the photon. The coherent-potential contribution reads

$$\tan\,\Theta_p = \frac{\bar{E}_x(L)}{\bar{E}_y(L)}, \tag{10}$$

where

$$\bar{E}_i(\vec{R}) = \int d\vec{R}'\langle G^R_{im}(\vec{R},\vec{R}')\rangle j_m(\vec{R}'). \tag{11}$$

The source term $\vec{j}(\vec{r})$ is chosen in such a way that the coherent part of transmitted electric field for $g=0$ equals

$$\bar{E}_i(\vec{r}) = \delta_{iy}e^{ik_0 z - z/2l}. \tag{12}$$

Using Eqs. (9) and (12), provided that $k_0 l \gg 1$, one finds

$$j_i(\vec{q}) = 2k_0(2\pi)^2 i\delta_{iy}\delta(q_x)\delta(q_y). \tag{13}$$

Substituting this expression into Eqs. (11) and (10) in the limits $g \ll 1$ and $k_0 l \gg 1$, we obtain

$$\tan\,\Theta_p = e^{ik_0 L}\left[\sin\frac{gk_0L}{2} - \frac{ig}{2}\cos\frac{gk_0L}{2}\right], \tag{14}$$

where $g \equiv g_z$. It follows from Eq. (14) that the coherent-potential approximation contribution, under the conditions $g \ll 1$ and $k_0 l \gg 1$, becomes inessential because it contains the strongly oscillating term $\exp(ik_0 L)$ when $k_0 L \gg 1$. Hence, any averaging over the wavelength of the incident photon will make this contribution negligible. Therefore, below, we concentrate our attention on the diffusional contribution to the Faraday rotation angle.

IV. DIFFUSIONAL CONTRIBUTION

Using Eq. (7), we have

$$I^D_{ij}(\vec{R},\vec{s}) = 2\int_0^\infty q^2 dq \int_{\vec{R}',\vec{r}',\vec{r},\vec{\rho}_1\cdots\vec{\rho}_4} e^{-iq\vec{s}\vec{r}} G^R_{im}(\vec{R}+\vec{r}/2,\vec{\rho}_1) G^A_{nj}(\vec{\rho}_3,\vec{R}-\vec{r}/2) \times P_{mnhs}(\vec{\rho}_1,\vec{\rho}_2,\vec{\rho}_3,\vec{\rho}_4) G^R_{hf}(\vec{\rho}_2,\vec{R}'+\vec{r}'/2) G^A_{gs}(\vec{R}'-\vec{r}'/2,\rho_4) j_f(\vec{R}'+\vec{r}'/2) j_g(\vec{R}'-\vec{r}'/2), \quad (15)$$

where $P_{mnhs}(\rho_1,\rho_2,\rho_3,\rho_4)$ is the sum of the ladder diagrams, which was found in innumerable papers, see, for example, Ref. [9]. We will calculate the intensity tensor in the limit $g \to 0$. Therefore, it is enough to calculate the diffusion propagator for $g = 0$. The main contribution to the integrals in Eq. (15) gives the term containing the diffusion pole. The corresponding mode has the form (see, for example, Ref. [9])

$$P_{mnhs}(\vec{\rho}_1,\vec{\rho}_2,\vec{\rho}_3,\vec{\rho}_4) = \delta_{mn}\delta_{hs}\delta(\vec{\rho}_1-\vec{\rho}_2)\delta(\vec{\rho}_3-\vec{\rho}_4)P(\vec{\rho}_1-\vec{\rho}_3), \quad (16)$$

where $P(\vec{\rho}) = \int \frac{d\vec{K}}{(2\pi)^3} P(\vec{K}) e^{i\vec{K}\vec{\rho}}$ and

$$P(\vec{K}) = \frac{3\gamma}{l/l_{\rm in} + K^2 l^2}. \quad (17)$$

Here, $l_{\rm in}$ is the inelastic mean-free path of a photon in the medium, and it is assumed that $\lambda \ll l \ll l_{\rm in}, L$.

Fourier transforming Eq. (15), substituting the expression $P(\vec{K})$ into it, and using Eq. (11), one obtains

$$I^D_{xy}(\vec{R},\hat{\mathbf{s}}_z) = 12\gamma l_{\rm in}\int_0^\infty q^2 dq \int_{-\infty}^\infty \frac{dK_z}{2\pi} \frac{e^{iK_z Z} G^R_{xm}(K_z/2+q) G^A_{my}(K_z/2-q)}{\left(1+K_z^2 l^2\right)\left(1+K_z^2 l l_{\rm in}\right)}, \quad (18)$$

where

$$G^{R,A}_{xm}(K_z/2+q) = \sum_{\alpha=\pm1} \frac{\frac{1}{2}(\delta_{xm} \mp i\alpha e_{xmz})}{(1-\alpha g_z)k_0^2 - (K_z/2+q)^2 \pm ik_0/l}. \quad (19)$$

The integral over K_z can be calculated exactly closing the integral contour in the complex K_z plane in the upper half ($Z > 0$). Note that the contributions from the poles $K_z = i/l$ and $K_z = i\sqrt{1/l l_{\rm in}}$ in the sum over polarizations cancel each other in the limits $g \to 0$ and $k_0 l \gg 1$. Substituting Eq. (19) into Eq. (18) and, subsequently, calculating the integrals over K_z and q, we obtain

$$I^D_{xy}(\vec{R},\hat{\mathbf{s}}_z) = 6\pi^2 \frac{l_{\rm in}}{l} e^{-Z/l} \sin\, g k_0 Z. \quad (20)$$

In deriving this expression, we assume that $g k_0 l \ll 1$, however, $k_0 l \gg 1$. The quantity $I^D_{yy}(\vec{R},\hat{\mathbf{s}}_z)$ can be calculated in the same way as $I^D_{xy}(\vec{R},\hat{\mathbf{s}}_z)$. In this case, the $g = 0$ approximation can be used because $I^D_{xy}(\vec{R},\hat{\mathbf{s}}_z)$ is already proportional to g. Substituting Eq. (11) into Eq. (18), one has

$$I_{yy}(\vec{R},\hat{\mathbf{s}}_z) = 4\pi^3 e^{-Z/l}. \quad (21)$$

Using the above-calculated expressions for $I^D_{xy}(\vec{R},\hat{\mathbf{s}}_z)$, $I^D_{yy}(\vec{R},\hat{\mathbf{s}}_z)$, and Eq. (8), we finally obtain the desired result for the Faraday rotation angle with the diffusional contribution,

$$\tan\,\Theta^D \approx \frac{3}{2\pi}\frac{l_{\rm in}}{l} \sin\, g k_0 L. \quad (22)$$

Equation (22) with Eq. (24) (see below) represent the central results of this paper. $\tan\,\Theta^D$ presents the asymptotically exact ($g \to 0$, $k_0 l \gg 1$) expression for the Faraday rotation in three-dimensional (3D) disordered systems. Comparing the two formulas $\tan\,\Theta^p$ and $\tan\,\Theta^D$, we see that the latter oscillates less due to the fact that $g \to 0$ in the argument of the sine function. Therefore, the diffusion contribution to the Faraday rotation Eq. (22) will dominate compared to the coherent-potential approximation contribution Eq. (14). This is valid provided that diffusional scattering is realized in the disordered system.

We are reminded that Eq. (22) has been derived assuming that $gL/l \ll 1$, however, gL/λ is not necessarily small. It is worth noticing that the ratio $l_{\rm in}/l$ is the average number of scatterings of the photon in the medium. If the thickness L of a slab is thinner than the length $\sqrt{l l_{\rm in}}$, then the diffusional trajectories are cut on the system size, and the above-mentioned number of scatterings becomes equal to L^2/l^2 (see Refs. [21,22]). In this particular case, Eq. (22) can be rewritten as

$$\tan\,\Theta^D \approx \frac{3}{2\pi T^2} \sin\, g k_0 L, \quad (23)$$

taking into account that, in the diffusional regime, the transmission coefficient T of a disordered slab is on the order of l/L. It follows from Eqs. (22) and (23) that the maximum of the Faraday angle is achieved at the frequencies where the photon elastic mean-free path l is minimal. In the case of Eq. (23) ($L < \sqrt{ll_{\rm in}}$), it is obvious that the maximum of the Faraday rotation corresponds to the minimum of the transmission coefficient and in its proximity. This type of dependence was confirmed experimentally in Refs. [15,16]. However, the Faraday rotation peak will be steeper because of stronger dependence on $l(\omega)$ (see below for more details). Another peculiarity of our result, Eq. (22), is that it implies an oscillating dependence on the rotation on g, that is, on a magnetic field, or the medium's internal properties. Note that the nonmonotonous dependence of the Faraday rotation on the magnetic field is observed in Ref. [17].

V. ROTATION IN THE BACKSCATTERED LIGHT: THE KERR EFFECT

For completeness, we now turn to the discussion of the Faraday rotation angle for the backscattered wave using the procedure outlined above. The main difference now is that one should take into account the contribution of the maximally crossed diagrams (Ref. [23]) in Fig. 2, which goes beyond the ladder diagram approximation, (i.e., regular diffusion). Another important point to mention is that, in the Kerr effect, the boundary conditions at $z = 0$ are important.

For a brief sketch of the derivation of the backscattering peak, note that the diffusion propagator P should fulfill the boundary condition at $z = 0$. Therefore, instead of the former P_{mnhs}, we, based on the method of images, use a modified $P(\vec{\rho},z_1,z_2) = P(\vec{\rho},z_1 - z_2) - P(\vec{\rho},z_1 + z_2)$. Here, $\vec{\rho}$ is a two-dimensional vector in the xy plane, and we assume that the following inequalities are met: $g \ll 1$, $k_0 l \gg 1$, and $gk_0 l \ll 1$. The details of the calculations of the backscattering rotation are given in Appendices A and B. The final result ($l_{\rm in} = \infty$, i.e., no absorption) reads

$$\tan\,\Theta_b^D = -\frac{3}{2}gk_0 l, \quad \tan\,\Theta_b^C = \frac{ig}{4}, \tag{24}$$

where $\Theta_b^{D,C}$ are the diffusional and maximally crossed diagram contributions to the Faraday rotation angle of the backscattered light, respectively. Note that maximally crossed diagrams lead to a pure imaginary Faraday angle, which indicates the onset of ellipticity for the backscattered wave. As seen from Eq. (24), the diffusional contribution is dominant in the diffusion regime $k_0 l \gg 1$ contrary to the maximally crossed diagram contribution, which becomes relatively large in the localized regime $k_0 l \sim 1$. In this regime $k_0 l \sim 1$, the diffusional and maximally crossed diagram contributions are on the same order, and a maximum of the rotation angle is achieved. Physically, such a behavior can be understood within the existing relation between the Faraday rotation angle and the time spent by the light in a medium [24,25] (see below). Indeed, in the diffusive regime, the backscattering time is longer for the low scatterer concentration (or for the larger photon mean-free path). With increasing the scatterer concentration (the photon mean-free path becomes smaller), the backscattering time increases because of the localization effects (or because of the ellipticity of the polarization of the reflected wave). This transparent picture serves as a basis for the qualitative understanding of the asymptotic behavior of the backscattered wave in two regimes. Thus, the onset of ellipticity in the backscattered wave can serve as a precursor of light weak localization.

Note that, in the limit $gk_0 l \gg 1$, the diffusional and maximally crossed diagram contributions to the rotation angle of the backscattering wave are very small [see Eqs. (A12) and (B16)]. Hence, for the backscattered wave, the maximal rotation is achieved for $g \sim 1/k_0 l$.

In concluding this section, let us estimate the traversal time of an electromagnetic wave in 3D disordered media. According to Ref. [24], the interaction time in a slab is closely related to the Faraday rotation. Hence, one might expect that the traversal time τ of an electromagnetic wave through a 3D disordered slab will be larger compared with the time $\tau_0 = Ln_0/c$ spent in a dielectric with open boundaries. Following Ref. [24], expanding Eq. (22) in powers of g, and keeping linear terms only, we get an estimated value for time $\tau \approx (l_{\rm in}/l)\tau_0$. Thus, the disorder enhanced the traversal time τ by an additional factor $l_{\rm in}/l$ in comparison with a free light propagation time τ_0.

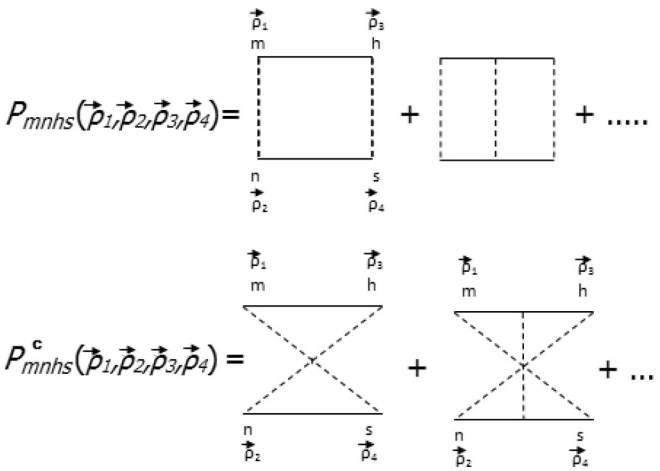

FIG. 2. The dashed line is the correlation function of random field Eq. (5), and the solid lines are the photon-retarded and advanced-averaged Green's functions Eq. (9).

VI. COMPARISON WITH THE EXPERIMENT

Most of the experiments on Faraday rotation in disordered media [13–17] are carried out with the films of thicknesses much less than the light wavelengths. Our approach cannot be applied directly to these systems because the randomness in this case is nearly two dimensional, contrary to our 3D randomness. We will compare our results with the experimental data of Ref. [18] where the sample has 3D randomness. First, let us estimate the dimensionless constant g for water noting that, in Ref. [18], nanoparticles are randomly embedded in the water. It follows from (19) that $g = (\varepsilon_+ - \varepsilon_-)/2 = n(n_+ - n_-)$ and $n = (n_+ + n_-)/2$. $\varepsilon_\pm$ and $n_\pm$ are

dielectric constants and refraction indices of right-hand and left-hand circularly polarized light at the 632-nm wavelength, respectively. The difference $\Delta n = n_+ - n_-$ is related to the Verdet constant ν: $\theta = \nu B L = \pi\, \Delta n\, L/\lambda$. Taking $B = 1$ T, one has $\Delta n = \lambda\nu/\pi$. For water at $\lambda = 632$ nm, $n = 1.33$ and $\nu = 3.4$ rad T^{-1} m^{-1}, see, for example, Ref. [26]. Therefore, $g = n\,\Delta n \sim 10^{-6}$. We see that, for water at $B = 1$ T, g is extremely small, and the limit $g \to 0$ in our theory is justified. The elastic photon mean-free path l in a system randomly embedded in a dielectric host medium of metallic spheres can be estimated as $l = 8\pi c^4/(9vf\omega^4)$, where v is the volume of a single sphere and f is the volume fraction of spheres in the medium [27]. We take $v \approx 4\pi a^3/3$, where $a \approx 85$ nm is the average size of the particles coated with gold in an aggregate state and $f = 0.035$ [18]. Substituting these values and $\lambda = 632$ nm into the expression of l, one gets $l \approx 5\lambda$. Now, let us estimate the inelastic mean-free path $l_{\rm in}$, which is defined as $l_{\rm in} = \lambda/(2\pi\, {\rm Im}\,\varepsilon_{\rm eff})$ [27,28] [${\rm Im}\,\varepsilon_{\rm eff} = 9f\varepsilon_2/(\varepsilon_1 - 1)^2$ is the imaginary part of the Maxwell-Garnett effective dielectric constant, and ε_1,ε_2 are the real and imaginary parts of the dielectric constant of gold at incident wavelength $\lambda = 632$ nm, respectively]. Taking $\varepsilon_1 \approx -10.7$ and $\varepsilon_2 \approx 3.23$, Ref. [29], one has $l_{\rm in} \approx 21.4\lambda$, and it is easy to convince oneself that the conditions for photon diffusion $\lambda \ll l(\lambda) \ll l_{\rm in}(\lambda) \ll L$ are realized in the experiment [18]. In this case, the additional large multiplier $l_{\rm in}/l \sim 4$ arises in the Verdet constant calculated within the effective Maxwell-Garnett theory. This additional factor could explain the discrepancy between the theoretical calculations and the experimental data, mentioned in Ref. [18]. Multiplying the Verdet constant of water 3.4 by $l_{\rm in}/l \sim 4$ and subtracting the water value, for the Verdet constant of the solution, one gets $\nu \sim 10.2$, which is in very good agreement with the corresponding experimental value [18].

VII. SUMMARY

We have investigated the Faraday rotation in a disordered medium. The rotation angle is calculated to the leading order of parameters $gk_0L, 1/k_0l$. It is shown that, in the diffusive regime, Faraday rotation is proportional to the ratio of the inelastic mean-free path $l_{\rm in}$ to the mean-free path l, that is, to the average number of photon scatterings in the medium. For the Faraday angle, the magnetic-field oscillating dependence is predicted. If the thickness L of a slab is thinner than the length $\sqrt{ll_{\rm in}}$, then the Faraday rotation is inverse proportional to the square of the transmission coefficient. The maximum rotation is achieved at frequencies where the photon elastic mean-free path is minimal. We have calculated the Faraday rotation of backscattered waves. Maximally crossed diagrams lead to an ellipticity of the backscattered wave. In the localized regime $k_0l \sim 1$, the diffusional and maximally crossed diagram contributions Eq. (24) to the rotation angle are on the same order. Therefore, the appearance of ellipticity in the backscattered wave can serve as a precursor of a weak localization of the light. In the backscattered wave, maximal rotation is achieved for $g \sim 1/k_0l$. Beyond this critical value, the rotation angle rapidly disappears. The traversal time of an electromagnetic wave through the slab is estimated in a diffusive regime. Comparison with the experimental data is carried out. To summarize, although the main result for Faraday rotation Eq. (22) is approximate, it, nevertheless, correctly predicts many of the peculiar features of most experimental results [13–18], discussed in this paper.

ACKNOWLEDGMENTS

We are grateful to T. Meyer, A. Akopian, and O. del Barco for helpful comments and discussions. V.G. acknowledges partial support by FEDER and the Spanish DGI under Project No. FIS2010-16430.

APPENDIX A: DIFFUSIONAL CONTRIBUTION TO THE KERR EFFECT

We first derive the diffusional contribution to the Kerr effect, i.e., $\tan\Theta_b^D = -\frac{3}{2}gk_0l$ of Eq. (24). To do this, let us note that the diffusional contribution to the intensity tensor, see Fig. 2, takes the form

$$I_{ij}^D(\vec{R},\vec{s}) = 2\int_0^\infty q^2dq \int d\vec{r}\, e^{-iq\vec{s}\vec{r}} \times \int d\vec{r}_1 d\vec{r}_2 G_{im}^R(\vec{R}+\vec{r}/2,\vec{r}_1) G_{mj}^A(\vec{r}_1,\vec{R}-\vec{r}/2) \times P(\vec{r}_1,\vec{r}_2)\bar{E}_h(\vec{r}_2)\bar{E}_h^*(\vec{r}_2), \quad \text{(A1)}$$

where

$$P(\vec{r}_1,\vec{r}_2) = P(\vec{\rho},z_1 - z_2) - P(\vec{\rho},z_1 + z_2). \quad \text{(A2)}$$

Here, $\vec{\rho}$ is the projection of $\vec{r}_1 - \vec{r}_2$ in the xy plane. $P(\vec{r})$ is determined by the three-dimensional Fourier transform of Eq. (17), and the coherent field $\bar{E}_h(\vec{r}_2)$ is determined by Eq. (12). Going through Fourier transforms in Eq. (A1), one gets

$$I_{ij}^D(\vec{R},\vec{s}) = 2\int_0^\infty q^2dq \int \frac{dq_{1z}dK_z}{2\pi}\delta(q_{1z} - K_z/2 - qs_z) \times G_{im}^R(q_{1z})G_{mj}^A(K_z - q_{1z})e^{iK_zZ}I(K_z), \quad \text{(A3)}$$

where

$$I(K_z) = \int_0^\infty dz_1dz_2P(0,z_1,z_2)e^{-iK_zz_1 - z_2/l}, \quad \text{(A4)}$$

and

$$P(0,z_1,z_2) = \int d\vec{\rho}\, P(\rho,z_1,z_2). \quad \text{(A5)}$$

Here, we assume that $s_\rho = 0$. Substituting Eqs. (17) and (A2) into Eq. (A5), we obtain

$$P(0,z_1,z_2) = \frac{3\gamma}{2l^2}[z_1 + z_2 - |z_1 - z_2|]. \quad \text{(A6)}$$

Note that the expression (A6) was derived by ignoring the absorption and assuming that $l_{\rm in} = \infty$. Substituting Eq. (A6) into Eq. (A4), one has

$$I(K_z) = \frac{3\gamma i}{K_z}(e^{-iK_zL} - 1) + \frac{3\gamma i}{K_z - i/l}. \quad \text{(A7)}$$

Note that, in order to arrive at Eq. (A7), we cut the diverging integral on the upper limit at the system thickness L. For the backscattered direction $s_z = -1$ and for $\vec{R} = 0$, the intensity

$I^D_{xy}(\vec{R},\vec{s})$ Eq. (A3) can be written in the form

$$I^D_{xy}(0,-1) = 2\int_0^\infty q^2 dq \int \frac{dK_z}{2\pi} G^R_{xm}(K_z/2-q) G^A_{my}(K_z/2+q) I(K_z). \tag{A8}$$

Substituting the Green's functions Eq. (9) into Eq. (A8) and keeping only linear terms on K_z, one has

$$I^D_{xy}(0,-1) = I(g) - I(-g), \tag{A9}$$

where

$$I(g) = i\int_0^\infty dq \int \frac{dK_z}{2\pi} \frac{I(K_z)}{\left(K_z + \frac{(1-g)k_0^2-q^2}{q} + \frac{ik_0}{ql}\right)\left(K_z + \frac{q^2-(1+g)k_0^2}{q} + \frac{ik_0}{ql}\right)}. \tag{A10}$$

We will integrate Eq. (A10) over K_z closing the integral contour in the bottom half of the complex plane where the function $I(K_z)$ has no poles. The contributions to the integral come from the poles $K_z = -\frac{(1-g)k_0^2-q^2}{q} - \frac{ik_0}{ql}$ and $K_z = -\frac{q^2-(1-g)k_0^2}{q} - \frac{ik_0}{ql}$. Using Eqs. (A7) and (A9) and taking the integral over K_z in the limit $g \to 0$, we find

$$\begin{aligned} I^D_{xy}(0,-1) = &-\frac{12g\gamma k_0^3}{l}\int_0^\infty \frac{q^2 dq}{\left\{\left[q^2-k_0^2(1-g)\right]^2 + k_0^2/l^2\right\}\left\{\left[q^2-k_0^2(1+g)\right]^2 + k_0^2/l^2\right\}} \\ &+ \frac{24g\gamma k_0^3}{l}\int_0^\infty \frac{q^2 dq}{\left\{\left[q^2-k_0^2(1-g)\right]^2 + 4k_0^2/l^2\right\}\left\{\left[q^2-k_0^2(1+g)\right]^2 + 4k_0^2/l^2\right\}}. \end{aligned} \tag{A11}$$

In Eq. (A11), by taking the remaining integrals over q in the limit $k_0 l \gg 1$, we finally obtain

$$I^D_{xy}(0,-1) = -\frac{9\pi\gamma l g k_0 l}{\left(2g^2k_0^2l^2+1\right)\left(4g^2k_0^2l^2+1\right)}. \tag{A12}$$

In the final step using Eq. (8) and dividing $I^D_{xy}(0,-1)$ by backscattered intensity at $g=0$, $I_{yy}(0,-1) = 3\pi\gamma l$ [9], we arrive at $\tan\Theta^D_b$ of Eq. (24) in the limit $gk_0 l \ll 1$.

APPENDIX B: MAXIMALLY CROSSED DIAGRAM CONTRIBUTION TO THE KERR EFFECT

In this Appendix, we derive the maximally crossed diagram contribution to the Kerr effect, i.e., $\tan\Theta^C_b = \frac{ig}{4}$ of Eq. (24). To this end, let us represent the maximally crossed diagram contribution, see Fig. 2, to the intensity tensor in the form

$$\begin{aligned} I^C_{ij}(\vec{R},\vec{s}) = 2\int_0^\infty q^2 dq \int_{\vec{r},\vec{r}_1,\vec{r}_2,\vec{\rho}_1\cdots\vec{\rho}_4} &e^{-iq\vec{s}\vec{r}} G^R_{im}(\vec{R}+\vec{r}/2,\vec{\rho}_1) G^A_{nj}(\rho_2,\vec{R}-\vec{r}/2) \\ &\times P^C_{mnhs}(\vec{\rho}_1,\vec{\rho}_2,\vec{\rho}_3,\vec{\rho}_4) G^R_{hl}(\vec{\rho}_3,\vec{r}_1) G^A_{fs}(\vec{r}_2,\vec{\rho}_4) j_l(\vec{r}_1) j^*_f(\vec{r}_2). \end{aligned} \tag{B1}$$

It follows from the symmetry, see Fig. 2, that

$$P^C_{mnhs}(\vec{\rho}_1,\vec{\rho}_2,\vec{\rho}_3,\vec{\rho}_4) = P_{mshn}(\vec{\rho}_1,\vec{\rho}_4,\vec{\rho}_3,\vec{\rho}_2). \tag{B2}$$

Note that, throughout the paper, we consider the maximally crossed and diffusion propagators P^C, P at $g=0$. The reason is that, in the weak-scattering limit $k_0 l \gg 1$, the main contribution gives the pole term which is unaffected by Faraday rotation or optical activity [10]. Using Eqs. (16) and (B2), one has, from Eq. (B1),

$$I^C_{ij}(\vec{R},\vec{s}) = 2\int_0^\infty q^2 dq \int d\vec{r}\, e^{-iq\vec{s}\vec{r}} \int d\vec{r}_1 d\vec{r}_2 G^R_{is}(\vec{R}+\vec{r}/2,\vec{r}_1) G^A_{hj}(\vec{r}_2,\vec{R}-\vec{r}/2) P(\vec{r}_1,\vec{r}_2) \bar{E}_h(\vec{r}_2) \bar{E}^*_s(\vec{r}_1). \tag{B3}$$

Going over to the two- and three-dimensional Fourier transforms in Eq. (B3) and using Eq. (12), we have

$$\begin{aligned} I^C_{xy}(0,\vec{s}) = 4\int_0^\infty q^2 dq \int_{-\infty}^{+\infty} \frac{dp_z}{2\pi} G^R_{xy}(q\vec{s}_\rho, p_z) G^A_{yy}(-q\vec{s}_\rho, p_z - 2qs_z) \\ \times \int_0^\infty dz_1 dz_2 P(|q\vec{s}_\rho|, z_1, z_2) \exp\left[-iz_1(p_z+k_0) + iz_2(k_0 - p_z + 2qs_z) - \frac{z_1+z_2}{2l}\right]. \end{aligned} \tag{B4}$$

We are reminded that $\vec{s}_\rho$ is the projection of the unit vector $\vec{s}$ on the xy plane. In the backscattered direction, $\vec{s}_\rho = 0$ and $s_z = -1$. Integrating Eq. (B4) consequentially over z_1 and z_2, we obtain

$$I^C_{xy}(0,-1) = 4\int_0^\infty q^2 dq \int_{-\infty}^{+\infty} \frac{dp_z}{2\pi} G^R_{xy}(p_z) G^A_{yy}(p_z+2q) F(p_z), \tag{B5}$$

where

$$F(p_z) = \frac{3\gamma i}{l^2(p_z + k_0 - i/2l)(k_0 - p_z + 2qs_z + i/2l)(-2p_z + 2qs_z + i/l)}. \tag{B6}$$

Substituting Eqs. (9) and (B6) into Eq. (B5), one has

$$I_{xy}^C(0,-1) = I_1(g) - I_1(-g) + I_2(g) - I_2(g), \tag{B7}$$

where

$$I_1(g) = -\frac{3\gamma}{2l^2}\int_0^\infty q^2 dq \int \frac{dp_z}{2\pi} \frac{1}{(p_z + k_0 - i/2l)(p_z - k_0 + 2q - i/2l)(p_z + 2q - i/2l)\left(p_z - \sqrt{(1+g)k_0^2 + ik_0/l}\right)}$$
$$\times \frac{1}{\left(p_z + \sqrt{(1+g)k_0^2 + ik_0/l}\right)\left(p_z + 2q - \sqrt{(1-g)k_0^2 - ik_0/l}\right)\left(p_z + 2q + \sqrt{(1-g)k_0^2 - ik_0/l}\right)}, \tag{B8}$$

and

$$I_2(g) = -\frac{3\gamma}{2l^2}\int_0^\infty q^2 dq \int \frac{dp_z}{2\pi} \frac{1}{(p_z + k_0 - i/2l)(p_z - k_0 + 2q - i/2l)(p_z + 2q - i/2l)\left(p_z - \sqrt{(1+g)k_0^2 + ik_0/l}\right)}$$
$$\times \frac{1}{\left(p_z + \sqrt{(1+g)k_0^2 + ik_0/l}\right)\left(p_z + 2q - \sqrt{(1+g)k_0^2 - ik_0/l}\right)\left(p_z + 2q + \sqrt{(1+g)k_0^2 - ik_0/l}\right)}. \tag{B9}$$

The square roots from the complex numbers are implied in the sense of the arithmetic root. In the next step, we expand these roots on g and $1/k_0 l$ up to the linear terms,

$$I_1(g) = -\frac{3\gamma}{2l^2}\int_0^\infty q^2 dq \int \frac{dp_z}{2\pi} \frac{1}{(p_z + k_0 - i/2l)(p_z - k_o + 2q - i/2l)(p_z + 2q - i/2l)(p_z - k_0 - gk_0/2 - i/2l)}$$
$$\times \frac{1}{(p_z + k_0 + gk_0/2 + i/2l)(p_z + 2q - k_0 + gk_0/2 + i/2l)(p_z + 2q + k_0 - gk_0/2 - i/2l)}, \tag{B10}$$

and

$$I_2(g) = -\frac{3\gamma}{2l^2}\int_0^\infty q^2 dq \int \frac{dp_z}{2\pi} \frac{1}{(p_z + k_0 - i/2l)(p_z - k_o + 2q - i/2l)(p_z + 2q - i/2l)(p_z - k_0 - gk_0/2 - i/2l)}$$
$$\times \frac{1}{(p_z + k_0 + gk_0/2 + i/2l)(p_z + 2q - k_0 - gk_0/2 + i/2l)(p_z + 2q + k_0 + gk_0/2 - i/2l)}. \tag{B11}$$

We calculate the integral over p_z closing the integral contour in the bottom half of a complex plane. The contribution for $I_1(g)$ comes from the residues of the following two poles:

$$\text{(i) } p_z = -k_0 - gk_0/2 - i/2l, \quad \text{(ii) } p_z = -2q + k_0 + gk_0/2 - i/2l. \tag{B12}$$

The result reads

$$I_1(g) = \frac{3i\gamma}{8k_0^2 l^2(gk_0 + 2i/l)}\int_0^\infty dq \frac{q + k_0}{(q - k_0 + gk_0/4 + i/2l)(q - k_0 - gk_0/4 - i/2l)}. \tag{B13}$$

Equation (B13) was derived by taking into account the fact that the main contribution to the integral on q gives the values that are close to k_0. Calculating the integral Eq. (B13) in the pole approximation, which is justified provided that $k_0 l \gg 1$, one has

$$I_1(g) = -\frac{3\pi\gamma}{2k_0^2 l^2}\frac{k_0}{(gk_0 + 2i/l)^2}. \tag{B14}$$

Correspondingly,

$$I_1(g) - I_1(-g) = \frac{12i\pi\gamma lg}{\left(4 + g^2 k_0^2 l^2\right)^2}. \tag{B15}$$

In an analogous manner, one can show that $I_2(g) - I_2(-g) = 0$. Therefore, using Eqs. (A9) and (B15), one finds

$$I_{xy}^C(0,-1) = \frac{12i\pi\gamma lg}{\left(4 + g^2 k_0^2 l^2\right)^2}. \tag{B16}$$

Similar to what was performed in Appendix A where $\tan\Theta_b^D$ was calculated, one readily sees that dividing $I_{xy}^C(0,-1)$ by backscattered intensity at $g = 0$, $I_{yy}(0,-1) = 3\pi\gamma l$ [9] yields $\tan\Theta_b^C$ of Eq. (24) in the limit $gk_0 l \ll 1$.

[1] P. W. Anderson, Phys. Rev. **109**, 1492 (1958).
[2] M. C. W. van Rossum and T. M. Nieuwenhuizen, Rev. Mod. Phys. **71**, 313 (1999).
[3] Y. Kuga and A. Ishimaru, J. Opt. Soc. Am. A **1**, 831 (1984).
[4] M. P. Van Albada and A. Lagendijk, Phys. Rev. Lett. **55**, 2692 (1985).
[5] P.-E. Wolf and G. Maret, Phys. Rev. Lett. **55**, 2696 (1985).
[6] M. Kaveh, M. Rosenbluh, I. Edrei, and I. Freund, Phys. Rev. Lett. **57**, 2049 (1986).
[7] Z. S. Gevorkian and Y. E. Lozovik, Phys. Scr. **56**, 208 (1997).
[8] M. Burresi, V. Radhalakshmi, R. Savo, J. Bertolotti, K. Vynck, and D. S. Wiersma, Phys. Rev. Lett. **108**, 110604 (2012).
[9] M. J. Stephen and G. Cwilich, Phys. Rev. B **34**, 7564 (1986).
[10] F. C. MacKintosh and S. John, Phys. Rev. B **37**, 1884 (1988).
[11] E. Prati, J. Electromagn. Waves Appl. **17**, 1177 (2003).
[12] M. S. Longair, *High Energy Astrophysics* (Cambridge University Press, Cambridge, UK, 1992).
[13] S. Tomita, T. Kato, S. Tsunashima, S. Iwata, M. Fujii, and S. Hayashi, Phys. Rev. Lett. **96**, 167402 (2006).
[14] R. Fujikawa, A. V. Baryshev, J. Kim, H. Uchida, and M. Inoue, J. Appl. Phys. **103**, 07D301 (2008).
[15] H. Uchida, Y. Masuda, R. Fujikawa, A. V. Baryshev, and M. Inoue, J. Magn. Magn. Mater. **321**, 843 (2009).
[16] H. Uchida, Y. Mizutani, Y. Nakai, A. A. Fedyanin, and M. Inoue, J. Phys. D: Appl. Phys. **44**, 064014 (2011).
[17] S. Tkachuk, G. Lang, C. Krafft, O. Rabin, and I. Mayergoyz, J. Appl. Phys. **109**, 07B717 (2011).
[18] R. K. Dani, H. Wang, S. H. Bossman, G. Wysin and V. Chikan, J. Chem. Phys. **135**, 224502 (2011).
[19] I. Crassee, J. Levallois, A. L. Walter, M. Ostler, A. Bostwick, E. Rotenberg, T. Seyller, D. van der Marel, and A. B. Kuzmenko, Nat. Phys. **7**, 48 (2011).
[20] T. C. Choy, *Effective Medium Theory* (Oxford University Press, Oxford, 1999).
[21] P. W. Anderson, Philos. Mag. B **52**, 505 (1985).
[22] Zh. S. Gevorkian, Phys. Rev. E **57**, 2338 (1998).
[23] J. S. Langer and T. Neal, Phys. Rev. Lett. **16**, 984 (1965).
[24] V. Gasparian, M. Ortuño, J. Ruiz, and E. Cuevas, Phys. Rev. Lett. **75**, 2312 (1995).
[25] V. Gasparian, T. Christen, and M. Büttiker, Phys. Rev. A **54**, 4022 (1996).
[26] A. Jain, J. Kumar, F. Zhou, L. Li, and S. Tripathy, Am. J. Phys. **67**, 714 (1999).
[27] S. John, Phys. Rev. B **31**, 304 (1985).
[28] K. Arya, Z. B. Su, and J. L. Birman, Phys. Rev. Lett. **57**, 2725 (1986).
[29] P. B. Johnson and R. W. Christy, Phys. Rev. B **6**, 4370 (1972).